Colloidal Metal Sulfide Nanoparticles for High Performance Electrochemical Energy Storage Systems

Duong Tung Pham[1,2], Ting Quan[1], Shilin Mei[3], Yan Lu[1,4]

Addresses

[1] Department of Electrochemical Energy Storage, Helmholtz-Zentrum Berlin für Materialien und Energie, 14109 Berlin, Germany

[2] School of Engineering Physics, Hanoi University of Science and Technology, No 1 Dai Co Viet Street, 100000 Hanoi, Vietnam

[3] School of Mechatronical Engineering, Beijing Institute of Technology, Beijing 100081, China

[4] Institute of Chemistry, University of Potsdam, 14476 Potsdam, Germany

Corresponding author: Yan Lu (yan.lu@helmholtz-berlin.de) and Shilin Mei (shilin.mei@bit.edu.cn)

Abstract

Transition metal sulfides have emerged as excellent replacement candidates of traditional insertion electrode materials based on their conversion or alloying mechanisms, facilitating high specific capacity and rate ability. However, parasitic reactions such as massive volume change during the discharge/charge processes, intermediate polysulfide dissolution, and passivating solid electrolyte interface formation have led to poor cyclability, hindering their feasibility and applicability in energy storage systems. Colloidal metal sulfide nanoparticles, a special class that integrates the intrinsic chemical properties of metal sulfides and their specified structural features, have fairly enlarged their contribution due to the synergistic effect. This review highlights the latest synthetic approaches based on colloidal process. Their corresponding electrochemical outcomes will also be discussed, which are thoroughly updated along with their insight scientific standpoints.

1. Introduction

Transition metal sulfides containing S^{2-}/S_2^{2-} dimers have attracted tremendous attention for electrochemical energy storage systems (EESs) because of their unique properties of high energy density, good conductivity, excellent stability, and vital catalyst functionalization feature.[1, 2] In addition, the massive resource of metal sulfides in natural mines offers scalable, low-cost, and sustainable active materials. However, the sulfides experience problems of structural degradation during metal-ion host (Li^+, Na^+, K^+) up-taking and extraction due to significant volume expansion/shrinking, causing severe capacity fading phenomena. Similar to the Li-S battery, full discharge-charge processes of lithium-ion batteries based on metal sulfides also can involve intermediate polysulfide anions. However, the effect of the dissolved polysulfide shuttling on their electrochemical performances has not been clearly identified yet.[3] Many research groups have aggressively tried to synthesize metal sulfides and conductive carbonous additives composites, which can significantly improve electrochemical performances.[4-8] In the light of this direction, functional metal sulfide materials based on colloidal routes with defined components and nanostructures are considered as excellent candidates for energy storage and conversion systems. Specifically, in the past few years, extensive effort has been reported on various forms of metals sulfide nanoparticles, such as nanospheres, nano cables, nanorods, and nanowires, to maximize the charge-storage capacity and improve the cycling performance.[3] Notably, the optimized structural property design of colloidal metal sulfide nanoparticles/nanocomposites has still been pursued with the advances in synthetic techniques. Such metal sulfide nanoparticles/nanocomposites are an ideal platform for studying the effects of the components, size, and morphology of electrode materials on their electrochemical performances.[9-11]

This mini-review aims to provide a state-of-the-art overview of the metal sulfides colloidal nanoparticles, which can work as electrode materials or high-efficiency electrocatalyst hosts for alkali rechargeable battery and supercapacitor devices within the last two years. In addition, the brief introduction of up-to-date synthetic strategies for metal sulfide@C composites with their compositions, structures, and corresponding performances are also summarized and represented herein. Along with that, the discussions of insight reaction mechanisms, side-effect issues, and prospective solutions are illuminated, targeting to actualize the use of metal sulfides in EESs technologies.

2. Design and synthesis of metal sulfides colloidal particles for electrochemical energy storage

The synthesis of metal sulfides with well-defined shapes, sizes, structures, and defect states has been intensively investigated, which is the initial step towards achieving high-performance energy storage systems. The strong dependence of high electrochemical performance on nanostructures has encouraged researchers to study the controllable synthesis of metal sulfides with tailored nanostructures. Among all methods, the colloidal method is of significant interest in both fundamental research and practical applications due to its unique features.

In general, the synthesis of metal sulfides using colloidal methods follows the dissolution-recrystallization mechanism.[12] Solvothermal/hydrothermal, precipitation and sulfidation synthesis are some of the most preferable methods because of their superiority in controlling the morphology of nanoparticles (Figure 1). Solvothermal/hydrothermal synthesis can be defined as a method for the synthesis of single crystals that depends on the solubility of minerals in hot solvent/water under high pressure. In this kind of synthesis, precursors of metal are used to allow a reaction with sulfide source

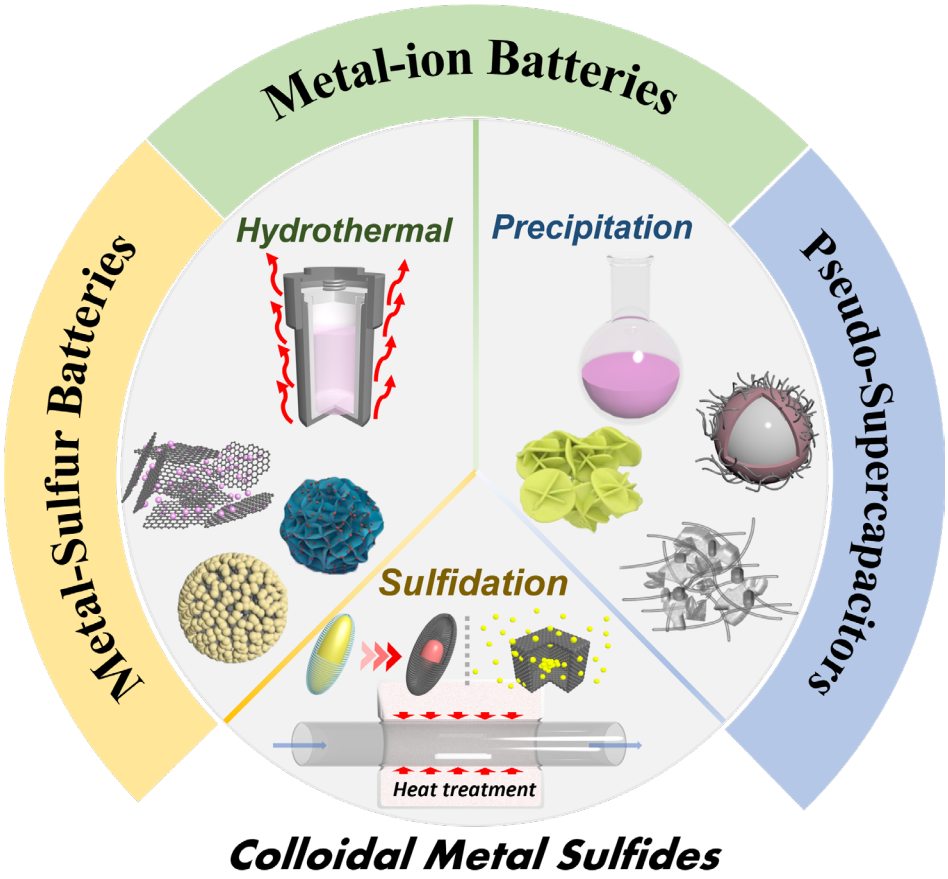

Figure 1. Colloidal routes for the synthesis of metal sulfide nanoparticles and their most popular applications in electrochemical energy storage systems.

materials or simply sulfur in an autoclave, where a sequence of physicochemical reactions take place under high temperature and pressure conditions. During the process, sulfide source can release H_2S when heated, which conjugates with metal ions and results in the formation of metal sulfide nanoparticles.[13, 14] The prepared metal sulfides nanoparticles are usually post-annealed at high-temperature under an inert atmosphere to increase their crystalline quality and purity. Figure 2a-c illustrates the preparation of MoS_2/amorphous carbon (C) microtubes (MTs) by Pan *et al.* via hydrothermal method using Sb_2S_3 microrod as a sacrificial template. [10] $Na_2S{\cdot}9H_2O$ and N_2H_4CS were used as sulfide source for Sb_2S_3 and MoS_2, respectively. The produced MTs consist of heterostructured MoS_2/C nanosheets, which were applied as cathode material for high performance Na-ion batteries.

Besides the mono-metal sulfides, hydrothermal/solvothermal method can also be used to synthesize bi-metal sulfides or multi-metal sulfides. For example, Tang *et al.*[15] takes advantage of the synergistic effect of hydrothermal method to synthesize Ni_2CoS_4/graphene oxide nanoparticles using $CoCl_2 \cdot 6H_2O$ and $NiCl_2 \cdot 6H_2O$ as the metal precursor and $Na_2S \cdot 9H_2O$ as the sulfur precursor. The synthesis was taken in the Teflon-lined stainless steel autoclave at 120 ^{o}C for 8 h.

Precipitation is another widely used method to synthesize metal sulfides nanoparticles in recent years. It is the creation of nanostructured materials as a powdered solid from a solution and allows the selection of the reaction conditions, where the nanostructured materials precipitate as a powdered solid from a

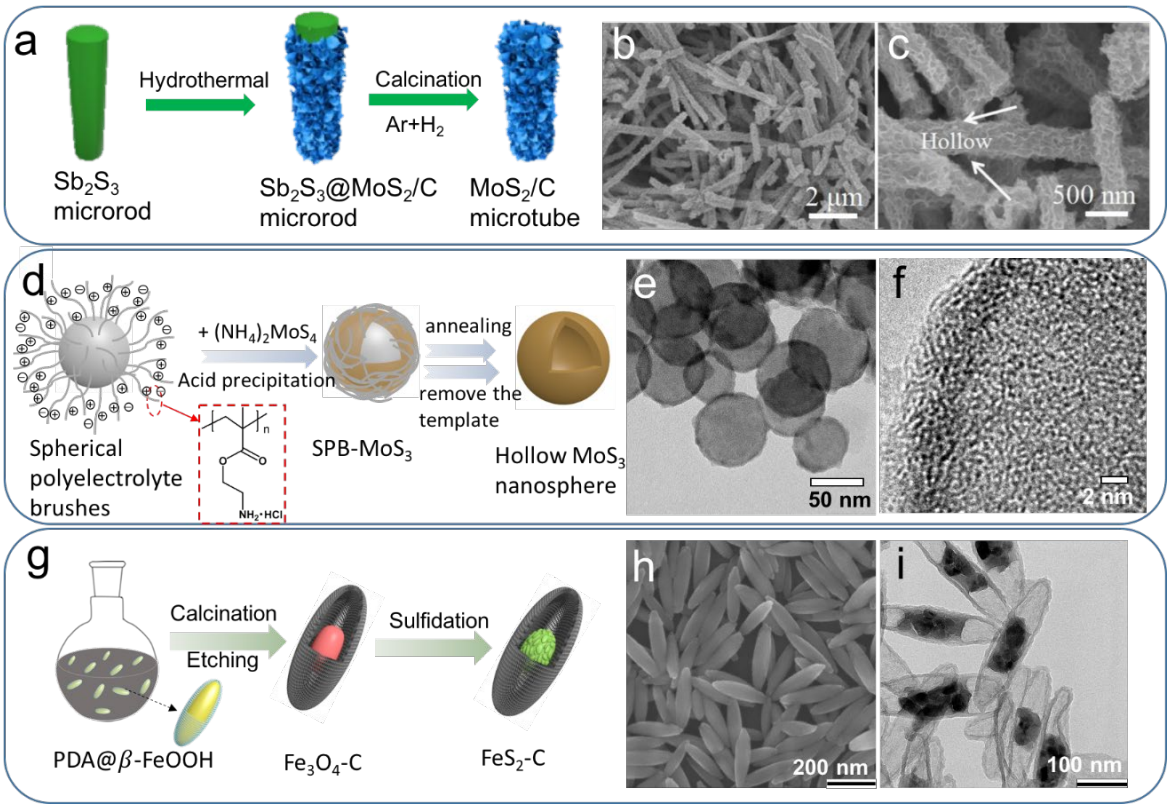

Figure 2. (a) Schematic illustration of the synthesis process and (b, c) SEM images of the MoS_2/C microtubes. Reproduced from ref. [13] with permission from American Chemical Society. *Copyright © 2018*. (d) Synthesis procedure and (e, f) TEM images of the hollow MoS_3 nanospheres synthesized by acid precipitation method. Reproduced from ref. [19]. (g) Synthesis procedure of the FeS_2-C nanospindles, (h) SEM image of the FeOOH nanospindles, and (i) TEM image of the FeS_2-C nanospindles. Reproduced from ref. [4]

solution. In the case of precipitation, which usually undergoes at room temperature, nano-sized crystals can be prepared in a highly pure and easily separate form. The common precipitates used to prepare metal sulfides are HCl, KOH, NaOH, ammonia, urea and tetramethylammonium hydroxide. In addition to the precipitants, some reductive and oxidative agents are often added to form metal sulfides.[16] In the final process, the precipitated metal sulfides can be heat treated by calcination or annealing to form the final product. A typical example of it is the synthesis of MoS_3 nanoparticles. As an alternative to MoS_2, MoS_3 has recently been widely explored as the electrode material for energy storage systems due to its unique one-dimensional chain structure and high electronic conductivity (bandgap of <1.5 eV).[17, 18] Quan *et al.*[19] reported the synthesis of hollow MoS_3 nanospheres using spherical polyelectrolyte brushes as soft template (Figure 2d-f), which follows the acid precipitation method with the reaction as: $MoS_4^{2-} + 2\ H^+ = MoS_3 \downarrow + H_2S \uparrow$, and the precipitated materials were heat-treated at 200 ^{o}C to form the final product.

Traditionally, metal sulfides can also be synthesized by the transformation from metal oxides. However, the obtained nanoparticles usually suffer from poor energy storage behavior due to the crucial transformation conditions. Recently, the sulfidation process and other methods have been widely used to convert metal oxides or hydroxides to metal sulfides, allowing the surface modification and morphology control of the final product. During the sulfidation process, sulfur powder is often used as the sulfur source. For instance, Xie *et al.*[4] prepared yolk-shell structured iron sulfide nanospindle (Figure 2g-i), where FeOOH acted as the iron source and provided the nanospindle structure. FeOOH was transformed to Fe_3O_4 via the first calcination under argon and then to FeS_2 during the second calcination process with sulfur powder at 400 ºC. This route uses the hard templates in aqueous solutions and provides a good way to control the morphology of the final product, which can only be realized by colloidal methods. The combination of hydrolysis and sulfidation methods provides the effective route to synthesize metal sulfides with uniform size, morphology and even good colloidal stability. Besides the sulfur powder, the direct addition of H_2S or a combination of H_2S during the heating treatment can also be used for the sulfidation synthesis of metal sulfides. The former one is usually used in synthetic routes where sulfur is absent in precursors, while the other one is for the precursors, which can act as both metal and sulfur precursors. Although the reactivity of H_2S is advantageous, it also presents numerous challenges to work with. To ensure safety, single‐droplet combustion experiments will have to be housed in a containment unit to be able to study these reactions.

Comparing different synthesis approaches, hydrothermal/solvothermal method is one of the best techniques to produce highly pure and nanostructured materials. It is much easier to control the properties of the synthesized materials by using different pressure and temperature conditions. However, the high temperature and pressure conditions make it very challenging to scale up the reactions. The precipitation technique is usually performed at room temperature and atmospheric pressure, which is easy to scale up the synthesis. But the surface modifications of the metal sulfides, such as carbon coating, cannot be realized at the same time by this method. Compared to them, sulfidation method is a unique technique as it transforms from the inactive metal oxide phase to an active sulfide phase, but the production process usually involves several steps, making the synthesis procedure complicated.

Up to now, a number of colloidal methods have been established to synthesize metal sulfides nanomaterials with high yield. However, some reaction mechanisms underlying the growth of different nanostructured metal sulfides, for example, nanobox, nanosphere, nanotube, remain unclear. Thus, the investigation of the reaction mechanisms behind the crystal growth route in order to search for suitable methods for different structures is of interest for future research. In addition, surface modification has been reported to enhance the properties of metal sulfides. There is still a high demand to develop facile synthesis approaches for the surface-functionalized metal sulfides with controlled size and morphology.

Table 1: Selected transition metal sulfides with detailed information on synthetic methods, morphology, and their electrochemical performances in various battery systems.

Compound and morphology	Synthetic method	Type of battery	Particle size	Electrode formulation/ mass loading	Performance	Rate capability (Capacity/ Current density)	Ref.
$Co_{1-x}S$ nanofibers	Electrostatic spinning and solvothermal	LIB	5−10 nm	Freestanding	~300 mAh g^{-1} at 2.0 A g^{-1}, 93% after 2000 cycles	527 mAh g^{-1}/ 0.5 A g^{-1} 470 mAh g^{-1}/ 1.0 A g^{-1}	[20]
$Co_{1-x}S$ hollow spheres	Solvothermal	LIB	~500 nm	80:10:10 (active material: carbon black: PVDF*)/ ~0.8 mg cm^{-2}	~538 mAh g^{-1} at 2.5 A g^{-1}, 67% after 100 cycles	572.5 mAh.g^{-1}/ 1.0 A g^{-1} 488.0 mAh g^{-1}/ 2.0 A g^{-1} 371.2 mAh g^{-1}/ 5.0 A g^{-1} 279.2 mAh g^{-1}/ 7.5 A g^{-1}	[6]
MoS_3 Hollow nanosphere	Acid precipitation	LIB	~100 nm	70:20:10 (active material: acetylene black: PTFE*) / 2.0 mg cm^{-2}	Full cell: ~89 mAh g^{-1} at 1.0 A g^{-1}, 75% after 100 cycles	80 mAh g^{-1}/ 0.5 A g^{-1} 49.7 mAh g^{-1}/ 2.0 A g^{-1}	[19]
NiS@rGO nanoparticle	Hydrothermal	LIB	15~25 nm	70:15:15 (active material: carbon black: CMC/SBR*)	~1328.7 mAh g^{-1} at 0.1 A g^{-1}, 75% after 100 cycles	835.8 mAh g^{-1}/ 0.5 A g^{-1} 752.1 mAh g^{-1}/ 1.0 A g^{-1} 673.6 mAh g^{-1}/ 2.0 A g^{-1} 538.1 mAh g^{-1}/ 5.0 A g^{-1}	[21]
FeS and FeS_2 microsphere	Gas-phase vulcanization approach	LIB/SIB	400-800 nm	80:10:10 (active material: CNT: PVDF*)/ 1.0 mg cm^{-2}	FeS_2@3DGF: ~889 mAh g^{-1} at 0.2 A g^{-1}, 50% after 140 cycles FeS@3DGF: ~1109 mAh g^{-1} at 0.2 A g^{-1}, 74% after 200 cycles	FeS_2@3DGF: 479 mAh g^{-1}/ 2.0 A g^{-1} 273 mAh g^{-1}/ 5.0 A g^{-1}	[22]
Fe_7S_8@, Co_9S_8@, Ni_9S_8@	Electro-blowing spinning and	LIB	~ 50 nm	Freestanding	Fe_7S_8@MPCNF: ~546 mAh g^{-1} at 1.0 A g^{-1}, 91% after 500 cycles	Fe_7S_8@MPCNF: 643 mAh g^{-1}/1.0 A g^{-1} 570 mAh g^{-1}/ 2.0 A g^{-1}	[7]

macro-porous carbon nanofiber	one-step sulfurization				Co_9S_8@MPCNF: ~654 mAh g^{-1} at 0.2 A g^{-1}, 87.7% after 200 cycles Ni_9S_8@MPCNF: ~459 mAh g^{-1} at 0.2 A g^{-1}, 80.1% after 200 cycles	Co_9S_8@MPCNF: 801 mAh g^{-1}/ 0.1 A g^{-1} 536 mAh g^{-1}/ 2.0 A g^{-} Ni_9S_8@MPCNF:614 mAh g^{-1}/ 0.1 A g^{-1} 392 mAh g^{-1}/ 2.0 A g^{-}	
Fe_3S_4/Co_9S_8 Hierarchical mulberry-like nanoparticles	Hydrothermal	LIB	600 nm	70: 20: 10 (active material: Super P: sodium alginate)	~945 mAh g^{-1} at 0.1 A g^{-1}, 71% after 100 cycles	698 mAh g^{-1}/ 0.5 A g^{-1} 643 mAh g^{-1}/ 1.0 A g^{-1} 574 mAh g^{-1}/ 2.0 A g^{-1}	[23]
Fe_3O_4/Fe_7S_8@C nanoparticles	Rapid rheological phase method	LIB	100-2000 nm	75:15:10 (active material: acetylene black: PVDF*) / 1.2 mg cm^{-2}	~945 mAh g^{-1} at 0.1 A g^{-1}, 71% after 100 cycles	825 mAh g^{-1}/ 0.5 A g^{-1} 778 mAh g^{-1}/ 1.0 A g^{-1} 717 mAh g^{-1}/ 2.0 A g^{-1}	[24]
Fe_3O_4/Fe_7S_8/C nanoplates	Hydrothermal	LIB	5–20 nm	70:20:10 (active material: Super P: CMC*) / 1.5 mg cm^{-2}	~514 mAh g^{-1} at 0.5 A g^{-1}, 93% after 350 cycles	511 mAh g^{-1}/ 1.0 A g^{-1} 358 mAh g^{-1}/ 5.0 A g^{-1} 283 mAh g^{-1}/ 10.0 A g^{-1}	[25]
CoS_2-MnS nanoparticles composites	Hydrothermal, and sulfidation	LIB	~25 nm	70:20:10 (active material: acetylene black: PVDF*)	~1324 mAh g^{-1} at 0.1 A g^{-1}, 88% after 100 cycles	1130 mAh g^{-1}/ 0.5 A g^{-1} 927 mAh g^{-1}/ 1.0 A g^{-1}	[26]
MoS_2@SnS anchored 3D carbon skeleton	Hydrothermal	LIB	5 nm	80:10:10 (active material: carbon black: CMC*) / 1.0–1.2 mg cm^{-2}	~831 mAh g^{-1} at 2.0 A g^{-1}, 93% after 1000 cycles	947 mAh g^{-1}/ 0.5 A g^{-1} 765 mAh g^{-1}/ 1.0 A g^{-1} 591 mAh g^{-1}/ 2.0 A g^{-1}	[16]
FeS@S and FeS_2@S yolk-shelled nanospindle	Hydrolysis and sulfurization	LSB	20-30 nm	80:10: 10 (active material: carbon black: PVDF*) / 1.0–1.1 mg cm^{-2}	FeS_2-C@S: ~761 mAh g^{-1} at 0.5 C, 86.7 % after 350 cycles FeS−C@S: ~537 mAh g^{-1} at 0.5 C, 63.9 % after 350 cycles	900 mAh g^{-1}/ 0.2 A g^{-1} 825 mAh g^{-1}/ 0.5 A g^{-1} 750 mAh g^{-1}/ 1.0 A g^{-1}	[4]

1T MoS_2@S and WS_2@S nanofiber	Solvothermal	LSB	200-300 nm	64:26:10 (active material: Ketjenblack: PVDF*)	MoS_2@S: ~900 mAh g^{-1} at 0.2 mA.cm^{-2}, 72% after 100 cycles WS_2@S: ~880 mAh g^{-1} at 0.2 mA.cm^{-2}, 72% after 100 cycles	MoS_2@S: 1000 mAh g^{-1}/2.0 mA.cm^{-2} WS_2@S:743 mAh g^{-1}/2.0 mA.cm^{-2}	[27]
FeS/N-C@S nanocomposite	Solution precipitation and one-step calcination	LSB	500 nm	80:10:10 (active material: Super P: PVDF*) / 1.7 mg cm^{-2}	~729 mAh g^{-1} at 0.5 C, 86.7 % after 500 cycles	1149 mAh g^{-1}/ 167.5 mA g^{-1} 729 mAh g^{-1}/1675 mA g^{-1} 570 mAh g^{-1}/3350 mA g^{-1} 335 mAh g^{-1}/5025 mA g^{-1}	[28]
MoS_2 /C tubular heterostructure	hydrothermal	SIB	300-400 nm	70:15:15 (active material: acetylene black: CMC*)	~493 mAh g^{-1} at 1.0 A g^{-1}, 81 % after 500 cycles	489.4 mAh g^{-1}/ 1.0 A g^{-1} 452.9 mAh g^{-1}/ 2.0 A g^{-1} 425.1 mAh g^{-1}/ 5.0 A g^{-1} 401.3 mAh g^{-1}/ 10.0 A g^{-1}	[13]
Fe_7S_8 nanospindle	solvothermal	SIB	<20 nm	70:15:15 (active material: Super P: PVDF*)	~450.8 mAh g^{-1} at 0.2 A g^{-1}, 66 % after 500 cycles	419.8 mAh g^{-1}/ 0.4 A g^{-1} 387.0 mAh g^{-1}/ 0.8 A g^{-1} 353.4 mAh g^{-1}/ 1.6 A g^{-1} 327.8 mAh g^{-1}/ 3.2 A g^{-1}	[29]
NiS_x 3D matrix	hydrothermal	SIB	1-20 nm	80:10:10 (active material: Super P: CMC*)/ ~0.5 mg cm^{-2}	~300 mAh g^{-1} at 1.0 A g^{-1}, 58.6 % after 800 cycles	520 mAh g^{-1} / 2.0 A g^{-1} 410 mAh g^{-1}/ 5.0 A g^{-1} 310 mAh g^{-1}/ 10.0 A g^{-1} 230 mAh g^{-1}/ 15.0 A g^{-1}	[8]
NiS Film composed of nanosheets	Silica-mediated conversion process	NIB	~150 nm	hybrid films	~407 mAh g^{-1} at 0.1 A g^{-1}, 58.6 % after 150 cycles	350 mAh g^{-1}/ 1.0 A g^{-1} 300 mAh g^{-1}/ 2.0 A g^{-1} 290 mAh g^{-1}/ 3.0 A g^{-1}	[30]

CoS_2 Multi-shelled Nanoboxes	Ion-conversion-exchange strategy	NIB	~800 nm	70:20:10 (active material: Super P: CMC*)/ 1.0 mg cm^{-2}	~509 mAh g^{-1} at 0.2 A g^{-1}, 95 % after 100 cycles	422 mAh g^{-1}/ 1.0 A g^{-1} 395 mAh g^{-1}/ 2.0 A g^{-1} 346 mAh g^{-1}/ 5.0A g^{-1}	[31]
Cu_2MoS_4 Hollow Nanospheres	Solvothermal	NIB	1-2 µm	80:10:10 (active material: carbon black: CMC*)/ ~1.0 mg cm^{-2}	~205.7 mAh g^{-1} at 0.5 A g^{-1}, 95.6 % after 2000 cycles	259.2 mAh g^{-1}/ 0.05A g^{-1} 40.3 mAh g^{-1}/ 5.0 A g^{-1}	[32]
SnS-SnSe2@3DC heterostructures	Spray-drying	NIB	200 nm	80:10 :10 (active material: carbon black: CMC*)/ ~ 0.8 mg cm^{-2}	580/100/100 ~580 mAh g^{-1} at 0.1 A g^{-1}, 90.2 % after 100 cycles	420 mAh g^{-1}/ 1.0 A g^{-1} 328 mAh g^{-1}/ 5.0 A g^{-1} 267 mAh g^{-1}/ 10.0 A g^{-1}	[33]
SnS_2@rGO Nanosheets	Solution precipitation	KIB	~ 100 nm	80:10:10 (active material: Super P: PAA*)/ 1.0–2.0 mg cm^{-2}	~ 387 mAh g^{-1} at 0.05 A g^{-1}, 87% after 100 cycles	355 mAh g^{-1}/ 0.2 A g^{-1} 289 mAh g^{-1}/ 0.5 A g^{-1} 247 mAh g^{-1}/ 1.0 A g^{-1}	[34]
$NiCo_{2.5}S_4$@rGO microrods	Sulfurization process	KIB	~ 4 nm	80:10:10 (active material: Super P: CMC*)/ 1.0 mg cm^{-2}	~495 mAh g^{-1} at 0.2 A g^{-1}, ~82% after 1900 cycles	507 mAh g^{-1}/ 0.2 A g^{-1} 472 mAh g^{-1}/ 0.5 A g^{-1} 442 mAh g^{-1} / 1.0 A g^{-1}	[35]
ZnS dendrites embedded nanorods	Solvothermal and sulfurization	KIB	~ 120 nm	90:10 (active material: PVDF*)/ 0.8−1.2 mg cm^{-2}	~330 mAh g^{-1} at 0.05 A g^{-1}, ~32% after 100 cycles	295 mAh g^{-1}/ 0.1 A g^{-1} 223 mAh g^{-1}/ 0.2 A g^{-1} 162 mAh g^{-1}/ 0.5 A g^{-1}	[36]
CuS@GO Nanosheet	Precipitation	KIB	~ 20–40 nm	80:10:10 (active material: carbon black: PVDF*)/ 0.8 mg cm^{-2}	~290.5 mAh g^{-1} at 0.1 A g^{-1}, ~71% after 100 cycles	291.4 mAh g^{-1}/ 0.3 A g^{-1} 256.2 mAh g^{-1}/ 0.5 A g^{-1} 196.5 mAh g^{-1}/ 1.0 A g^{-1}	[37]

Note: Lithium-ion battery (LIB), Lithium-Sulfur battery (LSB), Sodium-ion battery (NIB), Potassium-ion battery (KIB)

PVDF: poly(vinylidene fluoride); PTFE: poly(tetra fluoroethylene); CMC: carboxymethyl cellulose; SBR: Styrene-Butadiene; PAA: polyacrylic acid

Table 2. Selected transition metal sulfides on their synthetic methods, morphology, and electrochemical performances in supercapacitor application

Compound and morphology	Synthetic method	Particle size	Specific Surface area	Electrode formulation/ mass loading	Performance	Ref.
VS_4 3D sandwich structure	hydrothermal	50-70 nm	1890.1 m^2/g	80:10:10 (active material: carbon black: PVDF*)/ 4 mg cm^{-2}	497 F/g at 1 A/g, 64.7% after 5000 cycles at 1 A/g	[38]
CoS Flower-like hierarchitectures	hydrothermal	~2 μm	423.4 m^2/g	80:10:10 (active material: acetylene black: PTFE*) / 2 mg cm^{-2}	697 F/g at 1 A/g, 85.9% after 10000 cycles at 10 A/g	[39]
NiCoS nanoplate	co-precipitation and in situ sulfuration process	nanometers thickness	114.9 m^2/g	70:20:10 (active material: acetylene black: PVDF*)/2.1 mg cm^{-2}	758.9 F/g at 1 A/g, 63.6% after 10000 cycles at 10 A/g	[40]
Zn-Co-S microsphere	hydrothermal	~8 μm	106.8 m^2/g	Binder free/ 4.2 mg cm^{-2}	~149 mAh/g at 1 A/g, 81.4% after 6000 cycles	[41]
2D SnS_2 Nanorods	hydrothermal	an average length of about ~2-4 μm with a diameter of 20-60 nm	72.4 m^2/g	80:10:10 (active material: carbon black: PTFE*)/ 2 mg cm^{-2}	165.2 F/g at 3 A/g, 93% after 4000 cycles at 100 mV/s	[42]
Mesoporous NiCoMn-S	solvothermal	~100 nm	41.4 m^2/g	80:10:10 (active material: acetylene black: PTFE*)/ 4 mg cm^{-2}	661 F/g at 1 A/g, 86.5% after 1000 cycles	[43]

*: PVDF: poly(vinylidene fluoride)
PTFE: poly(tetra fluoroethylene)

3. Transition metal sulfide colloidal particles in electrochemical energy storage systems

3.1. Colloidal metal sulfides for high-performance metal-ion batteries

On the roadmap of developing better energy/power densities and excellent rate capability EESs, metal sulfides coupling with various doping compounds leads to novel nano-sized morphologies, significantly boosting the alkali metal host ($Li^+/Na^+/K^+$) diffusion sites and electronic conductivity.[44] Table 1 represents the updated works utilizing metal sulfides derived by various precursors and chemical synthesis processes. The details of nanoparticle size, electrode preparation, and their electrochemical outcomes are also included. It is worth pointing out that most systems could operate at high current rates, delivering excellent specific capacity and stability. These promising results are facilitated by the unique layered structure of the systems such as MoS_2, WS_2, ZrS_2, VS_2, VS_4, or SnS_2, containing the covalent bond between two-dimensional sandwiched S-Metal-S layers and held by the weak Van der Waals force.[45-47] The metal host ions can, therefore, be easily accommodated during the insertion process.[45] For example, molybdenum oxide-based materials (MoS_2 or MoS_3) are considered as one of the most promising candidates owning to their interesting electrochemical properties. It has been noted that the morphologies and particle size of them have significantly influenced the performances. High surface area MoS_3 hollow spheres facilitate ideal ion diffusion pathway and large electroactive sites suitable for battery/supercapacitor hybrid systems,[19] while MoS_2 anchored 3D carbon skeleton or tubular heterostructure provide robust insertion/exertion channels for long cycle life and high stability.[13, 16] In fact, the formation of host up-taking products $Li/Na/K_x$-MS_y is generally unstable, and they quickly decompose to metallic Li/Na/K and polysulfide species. These mechanisms lead to the significant expansion of layers, especially in the bulk-phase pristine metal sulfide particles.

Therefore, various structure/shapes (plate, sphere, mulberry, fiber, etc.) modification in nanoscale and proper doping/compositing with carbonaceous compounds could remarkably improve and reinforce diffusion pathways, which strongly enhances their electronic/ionic conductivities and structural stability of the composite, delivering superior high-rate performances.[25] Moreover, these new synthetic approaches could also reinforce interface kinetics during electrochemical processes, supporting remarkable rate and stable cyclability.[22] For instance, $Fe_3O_4/Fe_7S_8/C$ nanoplates,[25] MoS_2 /C nanosheets,[13] or NiS_x 3D matrix[8] can operate at >10 A g^{-1} current densities, retaining high discharge capacity in lithium, sodium, and potassium -ion batteries. Moreover, several studies created freestanding or self-supporting films with carbon nanofibers by colloidal physical/chemical processes.[7, 20] These composites demonstrate encouraging capacity retention after long cycling due to solid binding between nano-sized metal sulfide and carbon matrix. The composite/hybrid systems with polysulfide absorbers are also considered a promising approach to utilize each component feature. For example, Fe_3S_4/Co_9S_8,[23] Fe_3O_4/Fe_7S_8@C,[25] CoS_2-MnS,[26] and MoS_2@SnS[16] hybrid systems have achieved superior cycling ability and capacity retention.

Noted that the irreversible transformation of polysulfide and metallic compounds derives a new reaction of $A_2S + M/A_x \leftrightarrow S + M + A_{x+2}$ (A is alkali metal, M is transition metal) upon the subsequence cycles.[48] Unfortunately, these polysulfides are soluble in liquid electrolyte mediums, causing mass loss phenomena in the active electrode side and passivating layer formation in the reference electrode surface. Although recent reports have revealed stunning results of colloidal metal sulfide particles in EESs, effective strategies to compensate for these issues should be further addressed. Modifying the solid electrolyte interface (SEI) by different electrolytes, which could facilitate high compatibility to sulfide systems, may play a critical role in maintaining high cycle ability.

3.2. Catalytic metal sulfide for Metal-S batteries

Utilizing elemental sulfur as cathode and active metal (e.g., Li, Na, Mg, and Al) as anode, the rechargeable metal-sulfur batteries (RMSBs) enable a leap in specific energy owing to the high

theoretical specific capacity of both the metallic anode and the sulfur cathode.[49, 50] However, the shuttle effect led from highly soluble polysulfide intermediates and the sluggish kinetics of polysulfide conversion hinder the pragmatic application of RMSBs via rendering unstable cycling performances.[51] In this regard, metal sulfide nanoparticles designed and generated from colloidal routes stand out as efficient sulfur host due to the following advantages: (i) the sulfurphilic surface of metal sulfides enables a strong, but not exclusive binding to polysulfides, which can suppress the shuttle effect and preserve the intact configuration of polysulfides; (ii) metal sulfides show higher electronic conductivities than their oxide counterparts, some of which even exhibit half-metallic or metallic bonding; (iii) metal sulfides can serve as a catalyst for the conversion of polysulfides, which remarkably accelerates the redox reaction kinetics. Specifically, metal sulfide nanoparticles are far less limited by their ionic or electronic conductivities when compared to the bulk materials due to the very short internal diffusion paths. They can also withstand much greater mechanical deformation during charge/discharge processes, leading to prolonged cycling life.

Overall, these favorable effects significantly enlarge the variety of metal sulfide nanomaterials for RMSBs applications, especially in cathode development. Some representative works are listed in Table 1.[4, 22, 27, 28] In this direction, the strong adsorption of polysulfide intermediate is perceived as the major function of metal sulfide nanomaterials due to their sulfurphilic properties. For instance, Cui *et al*. systematically investigated the polysulfide adsorption capabilities of 7 candidate metal sulfides, revealing that TiS_2, FeS and MoS_2 exhibit greater polysulfide adsorption capabilities than Cu_2S, CuS, TiN, ZnS and CoS.[52] In addition, the catalyzing oxidation capability of metal sulfides is critical in reducing the energy barrier, leading to accelerated surface-mediated redox reaction and controlled Li_2S precipitation, therefore, contributes to the remarkably improved battery performance.[53] Particularly, the metallic 1T (octahedral) phase of metal sulfides exhibits a high electronic conductivity that is six orders of magnitude higher than that of 2H (hexagonal) phase, which can further catalyze the polysulfide conversion reactions.[54] In addition to the intrinsic advantages of metal sulfides, creating "sulfur deficiencies" is an innovative approach to suppress the shuttle effect.[55, 56] Taking MoS_{2-x} as an example, the sulfur deficiency results in larger charge densities on MoS_{2-x} (001) surface, finally promotes the corresponding thermodynamic and kinetic processes in the polysulfide conversion.[57]

Nevertheless, current studies of metal sulfide nanoparticles for RMSBs mostly focus on monovalent Li-S, K-S and Na-S batteries. The multivalent metal-sulfur systems, Mg-S, Al-S, and Ca-S, offer promising energy storage capabilities and better safety features as well. The research and development on these batteries is far behind the Li–S system due to many critical challenges. Future efforts and directions for both the fundamental and practical research are in great demand.

3.2. Supercapacitor

Metal sulfides, including layered and nonlayered types, are expected to meet the requirements for supercapacitors due to their rich redox reactivity than metal oxide counterparts.[58] The layered metal sulfides, such as MoS_2 and WS_2, are composed of three atom layers (S-M-S) bound by covalent bonds where the individual layers are held together by van der Waals forces, while the nonlayered ones, such as FeS_2 and ZnS, have chemical covalent bonds in three dimensions.[12] Both two types have attracted intensive research for supercapacitors in recent years due to their outstanding properties, such as good electrical conductivity, low electronegativity, high specific capacitance, high redox activity, and unique crystal structures.[59-61] The layered metal sulfides nanomaterials usually have high specific surface area due to their unique crystal structures, resulting in the high electrical double layer capacitance. Besides it, there is always intercalation followed by conversion process, which leads to high specific capacitance while undesirable cycling performance. Compared to it, only conversion process exists in nonlayered metal sulfides nanomaterials. For both of them, the relatively low electrical conductivity

and the large volume change during cycling are the most crucial problems that restrict their commercial use. Based on it, the combination of metal sulfides with conductive materials, or the growth of metal sulfides on conductive materials (carbon matrix) is an effective way to resolve the problems and has drawn great attention. For example, Maron *et al.*[60] fabricated a reduced graphene oxide/ multi-walled carbon nanotube-ZnS (rGO/MWCNTf/ZnS) hybrid 3D nanocomposite for supercapacitors. It was found that the addition of rGO improved the conductivity of the material, thus achieved high capacitance retention of up to 85% after 4000 cycles in symmetric two-electrode supercapacitors with 6 M KOH electrolyte.

Despite the efforts, the electrochemical performances of the combination of individual metal sulfides with carbon are still not satisfactory, which is ascribed to their structural damage in the electrochemical procedures resulting in fast capacitance fading. Therefore, many researchers are studying the bi- or multi-metal sulfides for supercapacitors. The synergetic effects between individual components will offset their respective drawbacks.

4. Conclusion and outlook

In summary, we provide an overview of the recent developments on the rational design and synthesis of metal sulfide nanoparticles as high-performance electrode materials for EESs. Great progress has been achieved in developing various types of metal sulfides from colloidal processes, forming desired compositions, morphologies, and properties. The advantageous effects of metal sulfide nanoparticles for different EESs involving metal-ion batteries, metal sulfur batteries, and supercapacitors are comprehensively discussed. Despite the encouraging progress in applying colloidal metal sulfides for advanced EESs, many challenges still exist due to the underlying complex electrochemical mechanism, which is still unclear and needs to be optimized. With continuous studies on metal sulfide nanoparticles and growing interest from battery communities, we anticipate that metal sulfide nanoparticles will play a vital role in energy storage applications in view of the unique structural and compositional features.

Declaration of interest: none

References

1. Xiao Y, Lee SH, Sun YK: **The Application of Metal Sulfides in Sodium Ion Batteries**. *Adv Energy Mater* 2017, **7**(3).
2. Stamenkovic VR, Strmcnik D, Lopes PP, Markovic NM: **Energy and fuels from electrochemical interfaces**. *Nat Mater* 2016, **16**(1):57-69.
3. Xu X, Liu W, Kim Y, Cho J: **Nanostructured transition metal sulfides for lithium ion batteries: Progress and challenges**. *Nano Today* 2014, **9**(5):604-630.
4. Xie DJ, Mei SL, Xu YL, Quan T, Hark E, Kochovski Z, Lu Y: **Efficient Sulfur Host Based on Yolk-Shell Iron Oxide/Sulfide-Carbon Nanospindles for Lithium-Sulfur Batteries**. *Chemsuschem* 2021, **14**(5):1404-1413.
5. Zhong W, Deng SB, Wang K, Li GJ, Li GY, Chen RS, Kwok HS: **Feasible Route for a Large Area Few-Layer MoS2 with Magnetron Sputtering**. *Nanomaterials-Basel* 2018, **8**(8).
6.* Liu SJ, Wang ZT, Zhang XH, He ZJ, Tong H, Li YJ, Zheng JC: **In Situ-Formed Hollow Cobalt Sulfide Wrapped by Reduced Graphene Oxide as an Anode for High-Performance Lithium-Ion Batteries**. *Acs Appl Mater Inter* 2020, **12**(2):2671-2678.

   The authors report $Co_{1-x}S$ hollow spheres formed by in situ growth on reduced graphene oxide layers, which exhibits excellent electrochemical performances in lithium ion battery. The

results illustrate that in situ growth on the graphene layers can enhance conductivity and restrain volume expansion of cobalt sulfide compared with ex situ growth.

7. Zhou XH, Su KM, Kang WM, Cheng BW, Li ZH, Jiang Z: **Locking metal sulfide nanoparticles in interconnected porous carbon nanofibers with protective macro -porous skin as freestanding anodes for lithium ion batteries**. *Chem Eng J* 2020, **397**.
8. Li SY, He W, Liu B, Cui JQ, Wang XH, Peng DL, Liu B, Qu BH: **One-step construction of three-dimensional nickel sulfide-embedded carbon matrix for sodium-ion batteries and hybrid capacitors**. *Energy Storage Mater* 2020, **25**:636-643.
9. Balakrishnan A, Groeneveld JD, Pokhrel S, Madler L: **Metal Sulfide Nanoparticles: Precursor Chemistry**. *Chemistry* 2021, **27**(21):6390-6406.
10. Jingjing Wang SL, Na Tian, Tianyi Ma, Yihe Zhang, and Hongwei Huang*: **Nanostructured Metal Sulfides: Classification, Modification Strategy, and Solar-Driven CO2 Reduction Application**. *Adv Funct Mater* 2020, **31**(9):2008008.
11. Stinn C, Allanore A: **Selective sulfidation of metal compounds**. *Nature* 2021.
12. Barik R, Ingole PP: **Challenges and prospects of metal sulfide materials for supercapacitors**. *Current Opinion in Electrochemistry* 2020, **21**:327-334.
13. Pan QC, Zhang QB, Zheng FH, Liu YZ, Li YP, Ou X, Xiong XH, Yang CH, Liu ML: **Construction of MoS2/C Hierarchical Tubular Heterostructures for High-Performance Sodium Ion Batteries**. *Acs Nano* 2018, **12**(12):12578-12586.
14. Chandrasekaran S, Yao L, Deng L, Bowen C, Zhang Y, Chen S, Lin Z, Peng F, Zhang P: **Recent advances in metal sulfides: from controlled fabrication to electrocatalytic, photocatalytic and photoelectrochemical water splitting and beyond**. *Chem Soc Rev* 2019, **48**(15):4178-4280.
15. Zhen Tang ST, Qiang Li, Zewei Wei, Tianli Zhou: **Synergistic effect of microwave heating and hydrothermal methods on synthesized Ni2CoS4/GO for ultrahigh capacity supercapacitors**. *J Colloid Interf Sci* 2020, **582**:312-321.
16. Ke GX, Chen HH, He J, Wu XC, Gao Y, Li YL, Mi HW, Zhang QL, He CX, Ren XZ: **Ultrathin MoS2 anchored on 3D carbon skeleton containing SnS quantum dots as a high-performance anode for advanced lithium ion batteries**. *Chem Eng J* 2021, **403**.
17. Chen H, Ke G, Wu X, Li W, Li Y, Mi H, Sun L, Zhang Q, He C, Ren X: **Amorphous MoS3 decoration on 2D functionalized MXene as a bifunctional electrode for stable and robust lithium storage**. *Chem Eng J* 2021, **406**.
18. Chu K NH, Li QQ, Guo YL, Tian Y, Liu WM: **Amorphous MoS3 enriched with sulfur vacancies for efficient electrocatalytic nitrogen reduction**. *J Energy Chem* 2021, **53**:132-138.
19.* Quan T, Xu YL, Tovar M, Goubard-Bretesche N, Li ZL, Kochovski Z, Kirmse H, Skrodczky K, Mei SL, Yu HT *et al*: **Hollow MoS3 Nanospheres as Electrode Material for "Water-in-Salt" Li-Ion Batteries**. *Batteries Supercaps* 2020, **3**(8):747-756.

In this work, hollow MoS_3 nanospheres were synthesized via a scalable room-temperature acid precipitation method. When applied in water-in-salt lithium ion battery, the prepared MoS_3 achieved a high specific capacity of 127 mAh/g at the current density of 0.1 A/g and good stability over 1000 cycles. These results demonstrated a novel routine for synthesizing metal sulfides with hollow structures using a template-based method and push forward the development of metal sulfides for aqueous energy storage applications.

20. Zhang XD, Zhao YR, Zhang CY, Wu CX, Li XP, Jin MJ, Lan W, Pan XJ, Zhou JY, Xie EQ: **Cobalt sulfide embedded carbon nanofibers as a self-supporting template to improve lithium ion battery performances**. *Electrochim Acta* 2021, **366**.
21. Ren HB, Wang JH, Cao YX, Luo W, Sun YF: **Nickel sulfide nanoparticle anchored reduced graphene oxide with improved lithium storage properties**. *Mater Res Bull* 2021, **133**.

22. Huang AM, Wang QQ, Ma ZY, Rui K, Huang X, Zhu JX, Huang W: **Surface Anionization of Self-Assembled Iron Sulfide Hierarchitectures to Enhance Capacitive Storage for Alkaline -Metal Ion Batteries**. *Acs Appl Mater Inter* 2019, **11**(43):39991-39997.
23. Liu Q, Chen ZZ, Qin R, Xu CX, Hou JG: **Hierarchical mulberry-like Fe3S4/Co9S8 nanoparticles as highly reversible anode for lithium-ion batteries**. *Electrochim Acta* 2019, **304**:405-414.
24. Tian H, Wu ZG, Zhong YJ, Yang XS, Guo XD, Wang XL, Zhong BH: **Rapid in-situ fabrication of Fe3O4/Fe7S8@C composite as anode materials for lithium-ion batteries**. *Mater Res Bull* 2021, **133**.
25. Chen K, Kong XZ, Pan AQ: **Sulfur-Doped Carbon-Wrapped Heterogeneous Fe3O4/Fe7S8/C Nanoplates as Stable Anode for Lithium-Ion Batteries**. *Batteries Supercaps* 2020, **3**(4):308-308.
26. Zheng J, He CJ, Li XC, Wang K, Wang TS, Zhang RT, Tang BHJ, Rui YC: **CoS2-MnS@Carbon nanoparticles derived from metal-organic framework as a promising anode for lithium-ion batteries**. *J Alloy Compd* 2021, **854**.
27. Eng AYS, Cheong JL, Lee SS: **Controlled synthesis of transition metal disulfides (MoS2 and WS2) on carbon fibers: Effects of phase and morphology toward lithium-sulfur battery performance**. *Appl Mater Today* 2019, **16**:529-537.
28. Li RR, Shen HJ, Pervaiz E, Yang MH: **Facile in situ nitrogen-doped carbon coated iron sulfide as green and efficient adsorbent for stable lithium-sulfur batteries**. *Chem Eng J* 2021, **404**.
29. Jin A, Kim MJ, Lee KS, Yu SH, Sung YE: **Spindle-like Fe7S8/N-doped carbon nanohybrids for high-performance sodium ion battery anodes**. *Nano Res* 2019, **12**(3):695-700.
30. Lu PY, Wang XW, Wen L, Jiang XT, Guo WL, Wang L, Yan X, Hou F, Liang J, Cheng HM *et al*: **Silica-Mediated Formation of Nickel Sulfide Nanosheets on CNT Films for Versatile Energy Storage**. *Small* 2019, **15**(15).
31.* Wang X, Chen Y, Fang YJ, Zhang JT, Gao SY, Lou XW: **Synthesis of Cobalt Sulfide Multi-shelled Nanoboxes with Precisely Controlled Two to Five Shells for Sodium-Ion Batteries**. *Angew Chem Int Edit* 2019, **58**(9):2675-2679.

In this work, yolk-shelled particles are gradually converted into cobalt divanadate multi-shelled nanoboxes by solvothermal treatment. Cobalt sulfide multi-shelled nanoboxes are produced through ion-exchange with S^{2-} ions and subsequent annealing. The as-obtained cobalt sulfide multi-shelled nanoboxes exhibit enhanced sodium-storage properties when evaluated as anodes for high performance sodium-ion batteries.

32. Chen JW, Mohrhusen L, Ali G, Li SH, Chung KY, Al-Shamery K, Lee PS: **Electrochemical Mechanism Investigation of Cu2MoS4 Hollow Nanospheres for Fast and Stable Sodium Ion Storage**. *Adv Funct Mater* 2019, **29**(7).
33.* Wang TS, Legut D, Fan YC, Qin J, Li XF, Zhang QF: **Building Fast Diffusion Channel by Constructing Metal Sulfide/Metal Selenide Heterostructures for High-Performance Sodium Ion Batteries Anode**. *Nano Lett* 2020, **20**(8):6199-6205.

The work confirms that the metal sulfide/metal selenide (SnS/SnSe2) hierarchical anode exhibits outstanding rate performance, where the normalized capacity at 10 A g^{-1} compared to 0.1 A g^{-1} is 45.6%. The proposed design strategy in this work is helpful to design high rate performance anodes for advanced battery systems.

34. Fang LZ, Xu J, Sun S, Lin BW, Guo QB, Luo D, Xia H: **Few-Layered Tin Sulfide Nanosheets Supported on Reduced Graphene Oxide as a High-Performance Anode for Potassium-Ion Batteries**. *Small* 2019, **15**(10).
35. Xie JP, Li XD, Lai HJ, Zhao ZJ, Li JL, Zhang WG, Xie WG, Liu YM, Mai WJ: **A Robust Solid Electrolyte Interphase Layer Augments the Ion Storage Capacity of Bimetallic-Sulfide-Containing Potassium-Ion Batteries**. *Angew Chem Int Edit* 2019, **58**(41):14740-14747.

36.* Chu JH, Wang WA, Feng JR, Lao CY, Xi K, Xing LD, Han K, Li Q, Song L, Li P *et al*: **Deeply Nesting Zinc Sulfide Dendrites in Tertiary Hierarchical Structure for Potassium Ion Batteries: Enhanced Conductivity from Interior to Exterior**. *Acs Nano* 2019, **13**(6):6906-6916.

In this work, zinc sulfide dendrites deeply nested in the tertiary hierarchical structure through a solvothermal-pyrolysis process are designed as an anode material for potasium ion battery. The architectural design of this material provides a stable diffusion path and enhances effective conductivity from the interior to exterior for both K^+ ions and electrons, buffers the volume expansion, and constructs a stable SEI during cycling.

37. Jia XX, Zhang EJ, Yu XZ, Lu BA: **Facile Synthesis of Copper Sulfide Nanosheet@Graphene Oxide for the Anode of Potassium-Ion Batteries**. *Energy Technol-Ger* 2020, **8**(1).
38. Wang XF, Zhang YF, Zheng JQ, Jiang HM, Dong XY, Liu X, Meng CG: **Fabrication of vanadium sulfide (VS4) wrapped with carbonaceous materials as an enhanced electrode for symmetric supercapacitors**. *J Colloid Interf Sci* 2020, **574**:312-323.
39. Ji ZY, Li N, Xie MH, Shen XP, Dai WY, Liu K, Xu KQ, Zhu GX: **High-performance hybrid supercapacitor realized by nitrogen-doped carbon dots modified cobalt sulfide and reduced graphene oxide**. *Electrochim Acta* 2020, **334**.
40. Luo YY, Tian YP, Tang Y, Yin XT, Que WX: **2D hierarchical nickel cobalt sulfides coupled with ultrathin titanium carbide (MXene) nanosheets for hybrid supercapacitors**. *J Power Sources* 2021, **482**.
41. Hekmat F, Hosseini H, Shahrokhian S, Unalan HE: **Hybrid energy storage device from binder-free zinc-cobalt sulfide decorated biomass-derived carbon microspheres and pyrolyzed polyaniline nanotube-iron oxide**. *Energy Storage Mater* 2020, **25**:621-635.
42. Sajjad M KY, Lu W: **One-pot Synthesis of 2D SnS2 Nanorods with High Energy Density and Long Term Stability for High-Performance Hybrid Supercapacitor**. *J Energy Storage* 2021, **35**.
43. Cao J, Hu Y, Zhu Y, Cao H, Fan M, Huang C, Shu K, He M, Chen HC: **Synthesis of mesoporous nickel-cobalt-manganese sulfides as electroactive materials for hybrid supercapacitors**. *Chem Eng J* 2021, **405**.
44. Zhao JB, Zhang YY, Wang YH, Li H, Peng YY: **The application of nanostructured transition metal sulfides as anodes for lithium ion batteries**. *J Energy Chem* 2018, **27**(6):1536-1554.
45. Xiao J, Wang XJ, Yang XQ, Xun SD, Liu G, Koech PK, Liu J, Lemmon JP: **Electrochemically Induced High Capacity Displacement Reaction of PEO/MoS2/Graphene Nanocomposites with Lithium**. *Adv Funct Mater* 2011, **21**(15):2840-2846.
46. Whittingham MS: **Lithium Incorporation in Crystalline and Amorphous Chalcogenides - Thermodynamics, Mechanism and Structure**. *J Electroanal Chem* 1981, **118**(Feb):229-239.
47. Py MA, Haering RR: **Structural Destabilization Induced by Lithium Intercalation in Mos2 and Related-Compounds**. *Can J Phys* 1983, **61**(1):76-84.
48. Fang XP, Guo XW, Mao Y, Hua CX, Shen LY, Hu YS, Wang ZX, Wu F, Chen LQ: **Mechanism of Lithium Storage in MoS2 and the Feasibility of Using Li2S/Mo Nanocomposites as Cathode Materials for Lithium-Sulfur Batteries**. *Chem-Asian J* 2012, **7**(5):1013-1017.
49. Salama M R, Attias R, Yemini R, Gofer Y, Aurbach D, Noked M: **Metal–Sulfur Batteries: Overview and Research Methods**. *ACS Energy Letters* 2019, **4**(2):436-446.
50.** Yu X, Manthiram A: **A Progress Report on Metal–Sulfur Batteries**. *Adv Funct Mater* 2020, **30**(39).

In this progress report, the fundamental principles of various metal–sulfur chemistries are first presented and compared. Then, the historical progress, recent advances, and key challenges of the Li–S, Na-S, Mg-S, Al-S, K-S, and Ca-S systems are summarized and discussed. Finally, future efforts and directions for both the fundamental and practical research are prospected.

51. Richter R HJ, Zhao-Karger Z, Danner T, Wagner N, Fichtner M, Friedrich KA, Latz A: **Degradation Effects in Metal–Sulfur Batteries**. *ACS Applied Energy Materials* 2021, **4**(3):2365-2376.

52.** Wu DS, Shi F, Zhou G, Zu C, Liu C, Liu K, Liu Y, Wang J, Peng Y, Cui Y: **Quantitative investigation of polysulfide adsorption capability of candidate materials for Li-S batteries**. *Energy Storage Mater* 2018, **13**:241-246.

The authors establish a standard procedure to quantitatively compare the polysulfide adsorption capability of candidate materials. They found that an order of magnitude of difference is evident between poor adsorption materials such as carbon black and strong adsorption materials such as V_2O_5 and MnO_2. The work provides a useful strategy to screen for suitable candidate materials and valuable information for rational design of long cycle life Li-S batteries.

53. Zhou G, Tian H, Jin Y, Tao X, Liu B, Zhang R, Seh ZW, Zhuo D, Liu Y, Sun J *et al*: **Catalytic oxidation of Li2S on the surface of metal sulfides for Li-S batteries**. *Proc Natl Acad Sci U S A* 2017, **114**(5):840-845.

54.* He J, Hartmann G, Lee M, Hwang GS, Chen Y, Manthiram A: **Freestanding 1T MoS2/graphene heterostructures as a highly efficient electrocatalyst for lithium polysulfides in Li–S batteries**. *Energy & Environmental Science* 2019, **12**(1):344-350.

The three-dimensional graphene/1T MoS_2 heterostructure is constructed by few-layered graphene nanosheets sandwiched by hydrophilic, metallic, few-layered 1T MoS_2 nanosheets with abundant active sites. The battery exhibited outstanding electrochemical performance, with a high reversible discharge capacity of 1181 mAh g^{-1} and a capacity retention of 96.3% after 200 cycles. The electrocatalysis mechanism is further experimentally and theoretically revealed, which provides new insights and opportunities to develop advanced Li–S batteries.

55. Lin H, Yang L, Jiang X, Li G, Zhang T, Yao Q, Zheng GW, Lee JY: **Electrocatalysis of polysulfide conversion by sulfur-deficient MoS2 nanoflakes for lithium–sulfur batteries**. *Energy & Environmental Science* 2017, **10**(6):1476-1486.

56. Liu M, Zhang C, Su J, Chen X, Ma T, Huang T, Yu A: **Propelling Polysulfide Conversion by Defect-Rich MoS2 Nanosheets for High-Performance Lithium-Sulfur Batteries**. *ACS Appl Mater Interfaces* 2019, **11**(23):20788-20795.

57. Zhang Q, Zhang X, Li M, Liu J, Wu Y: **Sulfur-deficient MoS2-x promoted lithium polysulfides conversion in lithium-sulfur battery: A first-principles study**. *Applied Surface Science* 2019, **487**:452-463.

58. Yuan H KL, Li T, Zhang Q: **A Review of Transition Metal Chalcogenide/Graphene Nanocomposites for Energy Storage and Conversion**. *Chin Chem Lett* 2017, **28**(12):2180-2194.

59. Kesavan D MV, Pazhamalai P, Krishnamoorthy K, Kim SJ: **Topochemically synthesized MoS2 nanosheets: A high performance electrode for wide-temperature tolerant aqueous supercapacitors**. *J Colloid Interface Sci* 2021, **584**:714-722.

60. Vaghasiya JV M-MC, Vyskocil J, Sofer Z, Pumera M: **Integrated Biomonitoring Sensing with Wearable Asymmetric Supercapacitors Based on Ti(3)C(2)MXene and 1T-Phase WS(2)Nanosheets**. *Adv Funct Mater* 2020, **39**(30):10.

61. Durga IK RS, Kalla RMN, Ahn JW, Kim HJ: **Facile synthesis of FeS2/PVP composite as high-performance electrodes for supercapacitors**. *J Energy Storage* 2020, **28**:8.